The Unrealized Potential of Superhydrophobic Substrates in Advanced Life Support Systems

Rawand M. Rasheed[1] and Mark M. Weislogel[2]
Portland State University, Portland, OR, 97201

Nearly all water processing equipment aboard spacecraft is to a large extent controlled by capillary forces arising from substrate wetting conditions. Superhydrophobic wetting conditions provide an essentially passive means to keep water away from certain substrates providing a level of no-moving-parts phase separation and control. This work presents a host of non-wetting aqueous microgravity capillary fluidics phenomena arising from interactions with easily fabricated superhydrophobic substrates. The value of such phenomena for potential life support applications aboard spacecraft is clear, especially for substrate properties that are thermally robust, corrosion resistant, and self-cleaning for both long- and short-term applications. Large length scale low-g demonstrations of the phenomena are provided in HD video format for the extensive drop tower tests conducted. The broader crosscutting impacts to numerous fluids processing operations for life support are discussed. Current practical applications addressed in light of superhydrophobicity include urine-processing, water recovery, fire safety, and others.

I. Introduction

In the absence of significant gravitational acceleration, multiphase fluid phenomena is controlled largely by surface tension and wetting conditions. The latter are characterized by the contact or wetting angle. Non-wetting conditions have not been exploited significantly aboard spacecraft to date despite their potential to passively repel and thus passively position liquids in highly advantageous ways. In this paper we provide a brief review of the literature regarding the terrestrial applications of superhydrophobic surfaces, including mention of examples found in nature and several theoretical foundations. We then provide a brief review of facile methods for producing such superhydrophobic substrates. Applications of such surfaces within the fluid systems aboard spacecraft are then discussed following demonstrations of large length scale superhydrophobic capillary phenomena in low-gravity drop tower experiments.

A class of substrates and surfaces that are strongly repellent to aqueous solutions are called superhydrophobic surfaces. Over the past 20 years, research into production methods of superhydrophobic surfaces has received significant attention for their use in a variety of applications including self-cleaning surfaces,[1-6] drag reduction,[7-9] anti-icing and anti-fog surfaces,[10-14] fouling-free surfaces,[15-17] fluid separation such as oil-water,[18,19] and corrosion protection for metals.[20,21] A special class of surfaces that are simultaneously repellent to aqueous solutions, oils, and alcohols are called superomniphobic surfaces.[22]

The wettability of a substrate is defined by the equilibrium contact angle θ, and the range of metastable contact angles above and below θ defined by contact angle hysteresis. Surfaces with contact angle above 150°, and low contact angle hysteresis, $< \pm 5°$, are classified as super-repellent, superhydrophobic surfaces. Figure 1 provides a common sketch for three equilibrium wetting conditions: wetting/partial wetting ($\theta < 90°$), neutral wetting ($\theta = 90°$), and non-wetting ($\theta > 90°$). A surface is considered superwetting when $\theta = 0°$. The equilibrium contact angle on a smooth surface has been defined by Young's relation

$$\sigma_{SV} = \sigma_{SL} + \sigma_{LV} \cos\theta, \tag{1}$$

where σ_{LV}, σ_{SV}, and σ_{SL} are the surface tensions of the liquid-vapor, solid-vapor, and solid-liquid, respectively. Figure 2 illustrates the interfacial force balance at the liquid-solid-gas contact line. According to Young's relation, to achieve large contact angles, the free surface energy σ_{SV} must be proportionally small. Young's relationship has an apparent theoretical limit of ~ 120° for water.[23,24] The maximum experimentally observed equilibrium water contact angle on a smooth surface observed in practice[25] is 130°.

Despite this apparent limit, many surfaces exist in nature that are superhydrophobic, with contact angles greater than 150°. The legs of water striders,[26-28] various plant leaves,[29-31] the eyes and wings of numerous insects,[32-34] and the

[1] Graduate Student/NSTRF Fellow, Mechanical and Materials Engineering, 1930 SW 4th Avenue
[2] Professor, Mechanical and Materials Engineering, 1930 SW 4th Avenue

backs of the Stenocara beetles[35-38] are all superhydrophobic. Oleophobic surfaces have also been observed in nature on the shells of Tetrodontophora Bilanensis and Orthonychiurus Stachianus, both soil dwelling arthropods.[39,40] The common feature allowing all of these organisms the enhanced ability to repel fluids is the presence of micro/nano-scale surface roughness. Wenzel[41] was perhaps the first to consider surface roughness effects on contact angle

$$\cos\theta^* = r\cos\theta, \tag{2}$$

where θ^* is the apparent contact angle and r is the roughness ratio defined as the ratio between the area of the rough surface to the area of the projected surface with no surface roughness, $r \equiv A_{rough}/A_{smooth}$. Figure 3a provides a schematic of a droplet on a rough surface in a Wenzel state. The Wenzel model considers a fluid that is in total contact with all surface features. The roughness ratio for a smooth surface is $r = 1$, and for a rough surface $r > 1$. It is apparent from Eq. 2, also known as the Wenzel model, that the roughness ratio enhances both wetting and non-wetting surface characteristics. That is, if $\theta < 90°$, $\theta^* < \theta$, but if $\theta > 90°$, $\theta^* > \theta$. The Wenzel model can predict droplet behavior in certain circumstances, but has limited value in others. The Wenzel model does not imply any upper limit on the roughness ratio, and does not take into consideration surface features of varying length scales.

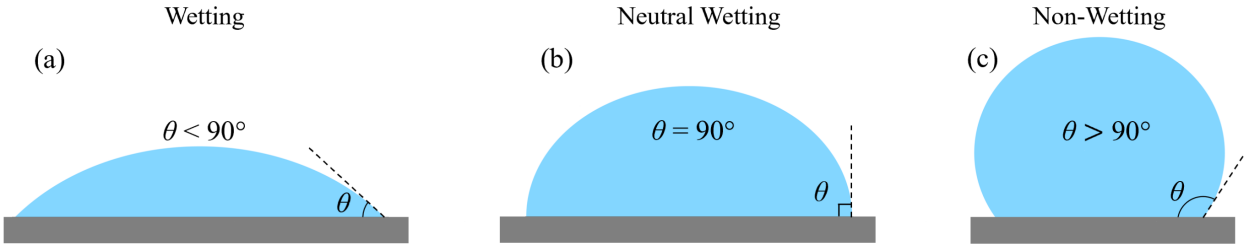

Figure 1: Liquid drop on a surface displaying (a) partial wetting, (b) neutral wetting, and (c) non-wetting states.

A second Cassie-Baxter model[42] takes into account n different surface features

$$\cos\theta^* = \sum_1^n f_i \cos\theta_i, \tag{3}$$

where f_i is an interfacial area fraction and θ_i the equilibrium contact angle predicted from Young's relation. Eq. 3 is a general form and can be simplified by recognizing that two characteristic interfacial area fractions exist such that $f_{i,LV} + f_{i,SL} = 1$, where $f_{i,LV}$ is the liquid-gas interfacial area fraction and $f_{i,SL}$ is the solid-liquid interfacial area fraction. Substituting $\cos\theta_{i,LV} = -1$, and assuming a homogenous material and a single characteristic roughness, the Cassie-Baxter model simplifies to

$$\cos\theta^* = f_{SL}(1 + \cos\theta) - 1. \tag{4}$$

Eq. 4 predicts the equilibrium contact angle of a droplet on a surface in the Cassie-Baxter state. The Cassie-Baxter model, unlike the Wenzel model, assumes that the liquid does not occupy the surface features. Instead, the liquid is only partially in contact with the solid. A liquid droplet in the Cassie-Baxter state is depicted in Fig. 3b. It can be shown via Eq. 4 that a fractional value for f_{SL} drastically increases the apparent contact angle. Surfaces that promote the Cassie-Baxter state have been used to achieve highly non-wetting characteristics with contact angles > 150° with low contact angle hysteresis < ± 5°, since the liquid droplet is in large part in contact with completely non-wetted air. Surfaces with more than one characteristic roughness feature are known as hierarchical surfaces, a feature that has been used to generate super-repellant surfaces that are superomniphobic.[43]

Thus, to achieve superhydrophobicity, a surface must have low surface energy, and must have at least one characteristic surface roughness length scale. Contact angle hysteresis is also a critical parameter for characterizing superhydrophobic surfaces. Contact angle hysteresis is defined as the difference in advancing, θ_A and receding, θ_R contact angles on a solid substrate, $\theta_A - \theta_R$. Shown in Fig. 4 is a stationary droplet on a tilted surface in a gravitational field with advancing and receding contact angles labelled. A surface with low contact angle hysteresis has a small difference between advancing and receding values. Droplets readily slide or roll across such surfaces with high contact angle and low contact angle hysteresis, whereas droplets on surfaces with a high contact angle and large contact angle

hysteresis move with an erratic stick-slip motion. Contact angle hysteresis arises from chemical and topographical variability in a surface. To achieve super-repellent surfaces, homogenous surface roughness and chemical composition are sought.

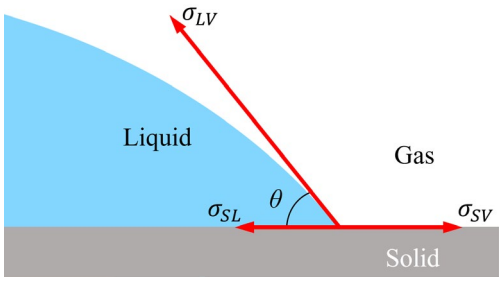

Figure 2: Force diagram of the three-phase contact line and relevant parameters for wetting.

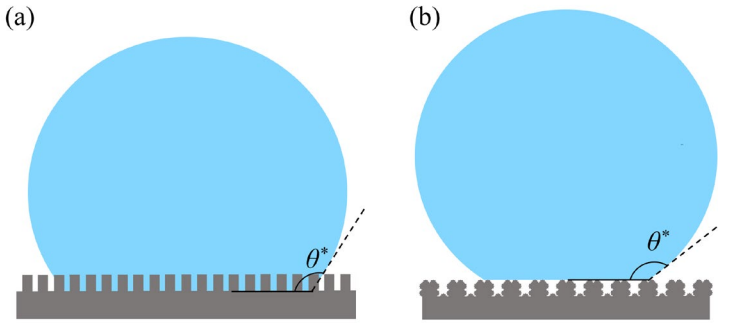

Figure 3: (a) A droplet on a rough surface in the Wenzel state. (b) A droplet in the Cassie-Baxter state on a hierarchically rough surface with a large surface roughness and a smaller secondary surface feature atop the larger surface roughness.

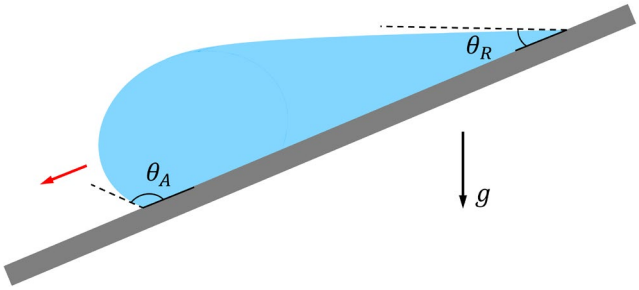

Figure 4: A droplet sliding on a surface with advancing contact angle, θ_A, and receding contact angle, θ_R.

Numerous advances have been made in the manufacture of superhydrophobic surfaces. There is a class of simple surfaces produced by chemical etch and immersion methods that provide an inexpensive means for producing superhydrophobic surfaces on metal substrates.[44] Such methods have the potential for production of superhydrophobic surfaces on complex geometries. Zhang et al.[45] developed an easy, one-step manufacturing process for the development of superhydrophobic surfaces on aluminum using a hydrochloric acid (HCl), ethanol, and myristic acid immersion method. The HCl chemically etches the aluminum surface, producing a hierarchically rough surface texture on the aluminum, while the myristic acid functionalizes the aluminum surface by depositing long chain, low-energy molecules (-CH_2 & -CH_3 groups) on the surface, rendering the aluminum superhydrophobic and exhibiting static water contact angles (SWCA) up to 160°. Wu et al.[46] highlight the increased reproducibility of aluminum superhydrophobic surfaces produced by acid etch and chemical functionalization. The use of an oxalic acid and HCl mixture for aluminum surface etching was found to produce a more homogenous microstructure. Li et al.[47] demonstrate added corrosion resistance to aluminum superhydrophobic surfaces by employing a potassium permanganate passivation step after acid etch and before an immersion coating step wherein the substrate is immersed in a solution of ethanol and 20 mM trichlorosilane. A superhydrophobic surface with SWCA of 153.5° and corrosion resistance to saltwater was produced. Other studies have employed modified versions of acid etching and surface functionalization seeking improved non-wetting capabilities as well as other unique substrate surface properties. Facile fabrication of aluminum surfaces with anti-icing characteristics,[48-52] surfaces functionalized using stearic acid for fluorine-free superhydrophobic surfaces relevant for environmentally friendly marine applications,[53,54] and surfaces that are thermally stable,[55] and others[56,57] have been developed using this method.

Facile coating methods have been employed for fabrication of superhydrophobic surfaces on various host substrates. Nanoparticles suspended in solutions that functionalize particles with low-energy coatings have been applied using curtain-coating,[58] electrospinning,[59] spin coating,[60] and dip coating methods.[61,62] Li et al.[63] produce superhydrophobic surfaces by brush coating a solution of titanium oxide nanoparticles modified in an ethanol-triethoxyoctylsilane solution. Gao et al.[64] produce superhydrophobic cotton surfaces by dip coating cotton in a solution of titanium oxide functionalized by n-octyltriethoxysilane. Spray coating methods have also been investigated for easy fabrication of superhydrophobic surfaces.[65-67] Li et al.[68] construct superhydrophobic surfaces on various substrates by spray coating a solution of amorphous silica nanoparticles, ethanol, and Trimethoxypropylsilane, achieving SWCA of

158.5°. Qahtan et al.[69] spray coat candle soot immersed in various solutions of acetone, isopropyl alcohol, and ethanol to produce superhydrophobic surfaces on metal substrates. Hancer & Arkaz[70] achieve SWCA greater than 178° on various substrates using a spray coated solution of silicon dioxide nanoparticles, functionalized by perfluorodecyltrichlorosilane, in a poly silicon matrix. Wei et al.[71] spray coat a mixture of silica nanoparticles, Methyltriethoxysilane, 3-[(Perfluorohexylsulfonyl) amino]-propyltriethoxysilane, and water on aluminum and glass substrates, producing syperhydrophobic surfaces that are also omniphobic, with SWCA of 158° and static contact angles of 148° and 134° for glycol and hexadecane, respectively. Chemical vapor deposition processes have also been studied for production of easy to produce superhydrophobic surfaces.[72-75]

Nearly all fluid systems aboard spacecraft are dominated by interfacial fluid phenomenon, which is to a large extent determined by substrate wetting conditions. Superhydrophobic surfaces have numerous applications for spacecraft water systems. Anti-fouling surfaces for fluid transport, liquid-gas and liquid-liquid passive phase separation, condensing heat exchanger surfaces,[76] and urine-water recovery are a few such applications. Herein, only facile methods for the production of superhydrophobic surfaces are outlined. Capillary fluidics experiments, conducted in the microgravity environment of a drop tower, demonstrating phenomenon arising from interactions with easily fabricated superhydrophobic surfaces are presented. Current applications of superhydrophobic surfaces for use in spacecraft fluid systems are discussed.

II. Experimental

A. Drop Tower and Function

A drop tower[77] is employed in this work to simulate microgravity conditions. An image of the facility is shown in Fig. 5. A touch screen computer allows a single operator to safely operate the drop tower assisted primarily by automated functions for quick experiment turn around, up to 20 drops per hour. An experiment rig is installed into a drag shield and released into freefall for 2.1 s. Figure 6 shows an example of an experiment rig inside the drag shield. The experiment rig and drag shield are released simultaneously. The drag shield is guided by two non-contacting cables. Two metal fins mounted to the sides of the drag shield pass through permanent magnets at the base of the tower. The relative motion between parallel magnetic fields and drag shield fins generate eddy currents in the fins that resist the motion and decelerate the falling masses which come to rest on foam pads. See Wollman[79] for further details.

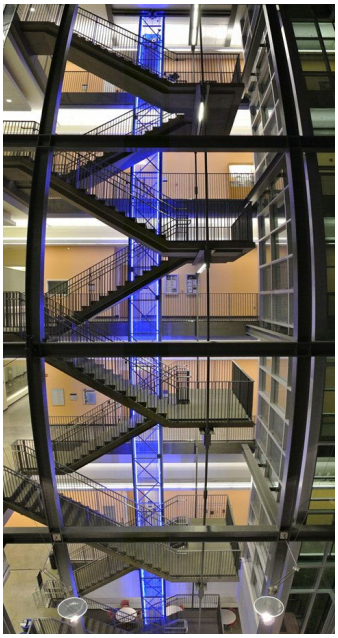

Figure 5: The 2.1 s drop tower. Image from Wollman and Weislogel.[79]

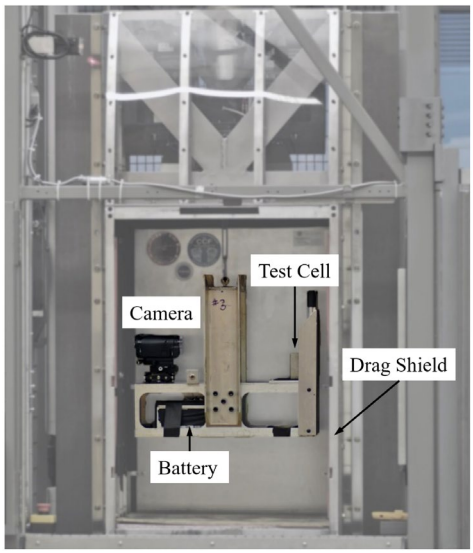

Figure 6: An experiment rig hanging inside the drag shield of the drop tower. Both the experiment rig and the drag shield are released at the same time. The experiment rig is allowed to fall freely inside the drag shield. Image from Torres.[80]

B. Production of Super-Facile Superhydrophobic Surfaces

Superhydrophobic surfaces requiring the most elementary of methods and materials for production have been developed and utilized in these studies. We define such surfaces as 'super-facile' surfaces. Superhydrophobic surfaces with SWCA of > 150° and roll off angles < 5° have been produced by spraying commercially available Dome Magic™ Polytetrafluoroethylene (PTFE) spray on sand paper of varying grit sizes (200-2000 grit). The PTFE spray is applied in three lapping passes 15 cm away from the substrate.

Cytonix WX2100™ one-step superhydrophobic spray is a commercially available product that is a fluorine-based spray that creates nanometer sized surface features. Shown in Fig. 7a is a scanning electron microscope (SEM) image

showing the surface with nanometer-scale features. Rust-Oleum Neverwet™ spray is another commercially available solution, a silicon-based spray that also forms nanometer-scale features, as shown in Fig. 7b. Both sprays provide similar ease of application and performance for purposes of the present demonstrations.

A super-facile production method of a thermally stable superhydrophobic surface has been employed for high-temperature applications. A surface is coated with candle soot until completely blackened. The surface is then sprayed with Dome Magic™ PTFE spray in two to three lapping passes 15 cm away from the substrate. The PTFE spray acts as a binder for the fragile soot producing a mechanically robust surface that is also thermally stable. This surface has been repeatedly used in experiments where surface operating temperatures exceed 220°C with negligible losses in wetting characteristics.

III. Low-g Demonstrations and Applications

A. Liquid Rebounds from Superhydrophobic Surfaces

A host of drop tower experiments have been conducted demonstrating and investigating large length scale interfacial fluid phenomenon arising from interactions with superhydrophobic surfaces. In a microgravity environment, the length over which capillary forces are significant increases 1000-fold leading to enormous surface tension-dominated phenomena dictated often by the nanoscale wetting conditions of the system. For example, Attari et al.[81] demonstrate that large droplets (puddles) deposited on superhydrophobic surfaces in a terrestrial gravity environment spontaneously jump when experiencing a step reduction in gravity. This phenomenon has been coined 'puddle jumping.' Figure 8 shows a series of images of a 2 mL water puddle jumping from a superhydrophobic surface in the microgravity environment of a drop tower. Upon experiencing a step reduction in gravity (a) the puddle reorients into a sphere, resulting in (b) a collision of capillary waves, which overcome the negligible adhesion forces between the fluid and superhydrophobic substrate, resulting in the puddle (c) detaching from the surface with (d-e) constant velocity despite a variety of oscillation modes.

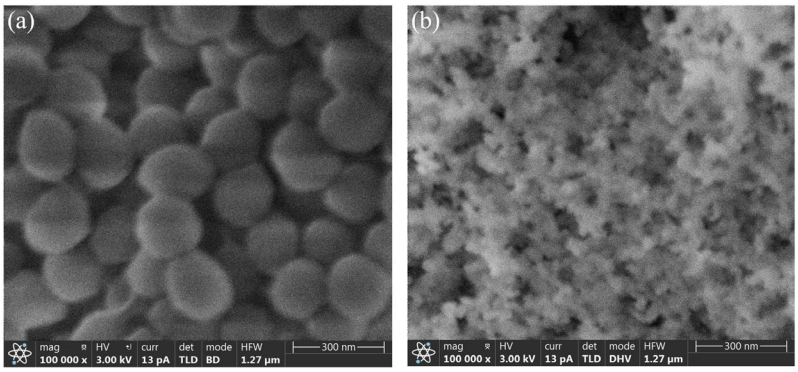

Figure 7: SEM images of (a) Cytonix WX2100™ and (b) Rust-Oleum Neverwet™ surface coatings.

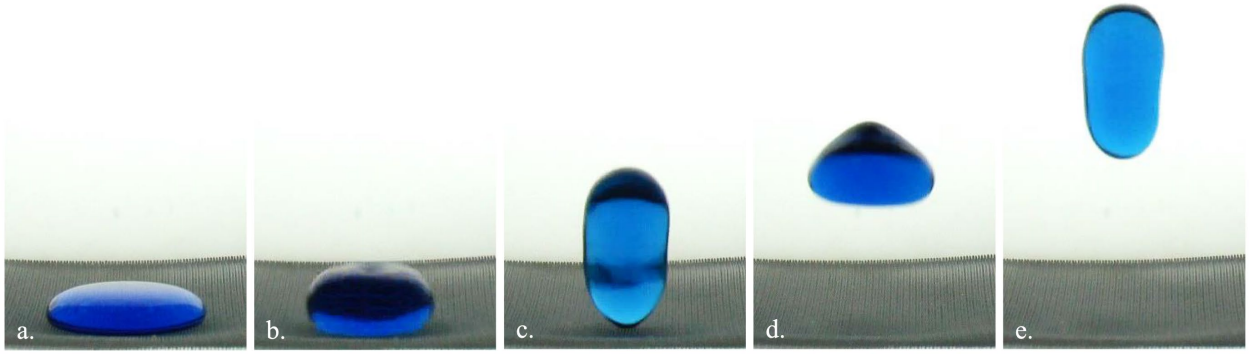

$t = 0$ s 0.05 0.13 0.23 0.37

Figure 8: (a) A 2 mL puddle of water flattened under the force of gravity. (b) The droplet reorients into a sphere in microgravity. (c) Collision of capillary waves due to droplet reorientation propel the droplet off the surface with constant velocity and vertical modes of oscillation (d) & (e).[81]

Puddle jumping phenomenon is a convenient droplet deployment method that has been applied in numerous microgravity experimental works including quantifying electrostatic forces on droplets[83] and droplet impact experiments,[78] such as dynamic Leidenfrost impacts.[81] However, droplet oscillations produced during the puddle

jumping process are undesirable for experiments sensitive to droplet oscillation modes at impact. A microgravity, oscillation-free, droplet generator, referred to as a 'Logan Shooter,' is a device that was developed for passive non-oscillating drop deployment.[80,84,85] Figure 9a shows a schematic of the shooter. The Logan Shooter consists of two superhydrophobic surfaces forming a wedge. A volume of water is dispensed near the narrowest point of the wedge. Large liquid volumes form puddles. At initiation of the drop tower test the 'puddle' jumps from the surface in an attempt to establish a sphere. However, the water is confined by the wedge which induces a capillary pressure gradient in the confined droplet that drives it out of the wedge. Oscillations in the drop are substantially damped during the ejection process. Figure 9b shows a Logan Shooter with 5° wedge half-angle ejecting a 10 mL droplet of water free of oscillations. Figure 10 shows a 30 Hz image overlay of a 1 mL droplet of water ejected between two parallel superhydrophobic plates using a Logan Shooter. The plates are separated by a distance of 13.5 mm, with overall length of 127 mm. The droplet has an initial velocity of 31.9 cm/s and final velocity of 23.2 cm/s. The sum of incident and reflection angles, $\theta_i + \theta_r$, increase from 93° to 100° over the course of five bounces.

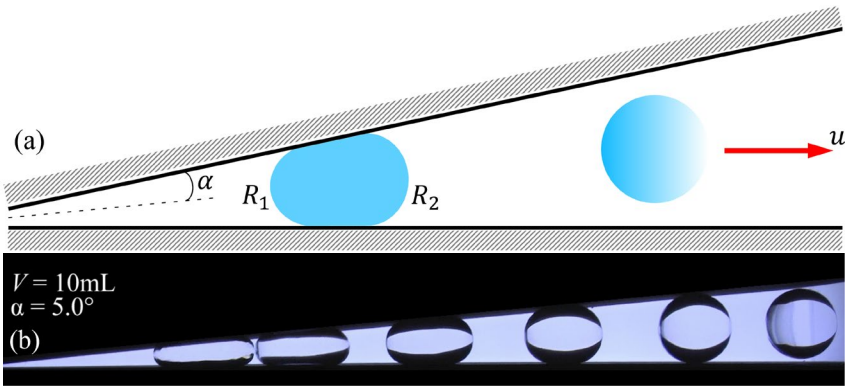

Figure 9: (a) A schematic of the Logan Shooter with half angle, α, and a droplet confined between two superhydrophobic plates. A capillary pressure gradient arising from the disparity in posterior and anterior radii of curvature, R_1 and R_2, respectively, forces the droplet out of the wedge with a velocity, u. (b) A Logan Shooter with 5° half-angle ejecting a 10-mL droplet of water.[80]

Figure 10: A 30 fps overlay image of a 1 mL water droplet ejected with a Logan Shooter between two superhydrophobic plates. Plates are separated by a distance of 13.5 mm with total length of 127 mm. The droplet velocity decreases from 31.9 cm/s to 23.2 cm/s and $\theta_i + \theta_r$ increase from 93° to 100° over the course of five bounces.

Jet impacts on superhydrophobic surfaces in microgravity have been studied extensively.[86-89] Figure 11 shows an image of a large jet impacting a superhydrophobic surface in microgravity. The 6 mm diameter jet impacts with a Weber number defined as the ratio of inertial to surface tension forces $We = \rho u^2 D/\sigma = 21.4$ and a Reynolds number defined as the ratio of inertial to viscous fluid forces $Re = \rho u D/\mu = 3005$. The incoming impact angle is 17.6° resulting in a perpendicular Weber number of 1.9. The jet is flattened upon impact due to inertial forces and rebounds into a cylindrical jet due to surface tension forces. In effect, the jet bounces off the surface. Such impacts have been studied extensively,[86] mapping stable and unstable impact regimes.

Figure 11: A large 6 mm jet impacting and rebound from a superhydrophobic surface in a low-gravity environment. Image from Cardin.[86]

B. Inhibition of Surface Fouling During Microgravity Transport of Aqueous Fluid Streams

The wetting characteristics of many aqueous solutions on superhydrophobic surfaces are often similar to those of pure water. Figure 12 provides a plot of contact angles for water, urine, and aqueous solutions of 25 g/L NaCl, sugar

and KCl on a superhydrophobic surface consisting of candle soot and Dome Magic™ PTFE spray applied to an aluminum substrate. All of the liquids exhibit contact angles > 150° and are within the standard error of water contact angle measurements.

Transport of waste-water streams in microgravity has proven a challenging problem due to biofouling surfaces on system components and plumbing; i.e., urine streams.[90-92] The non-wetting characteristics of urine on superhydrophobic surfaces offers attractive opportunities for applications of non-wetting surfaces to separate, contain, and transport urine streams in microgravity. As an example, an experiment modelling the current operating conditions of the urinal funnel and hose system of the ISS potty was conducted.[96,97] Two half-sections of 5.08 cm ID polyvinyl chloride (PVC) pipe were used in the tests. The inside of one half-section was coated with a superhydrophobic coating. Figure 13a provides a schematic of the experiment. A 100 mL volume of urine is poured into the half-pipe at a flowrate of 1 Lpm. The experiment is repeated every two to three hours for over one month. Figure 13b shows an image of the superhydrophobic half-pipe interior (above) and the non-hydrophobic half-pipe interior (below) after the first day of experimentation. A red box over a region on the non-hydrophobic half-pipe (Fig. 13b, bottom) shows initial signs of dry discolored urine residue on the non-hydrophobic pipe. Figure 13c shows an image of the same pipes after 31 days of testing. Discoloration of the uncoated pipe appeared at the first day of testing. The first signs of contamination for the superhydrophobic half-pipe were not detected until the 31st day of testing (see red boxes). Mass measurements of the PVC pipes over the span of 42 days of experimentation show an average increase in mass of 3.1 mg per experiment for the non-hydrophobic half-pipe, and an average increase in mass of 0.5 mg per experiment for the superhydrophobic half-pipe. These preliminary results demonstrate what might be crudely approximated as 30-fold increase in surface life for the superhydrophobic surface compared to the non-hydrophobic surface.

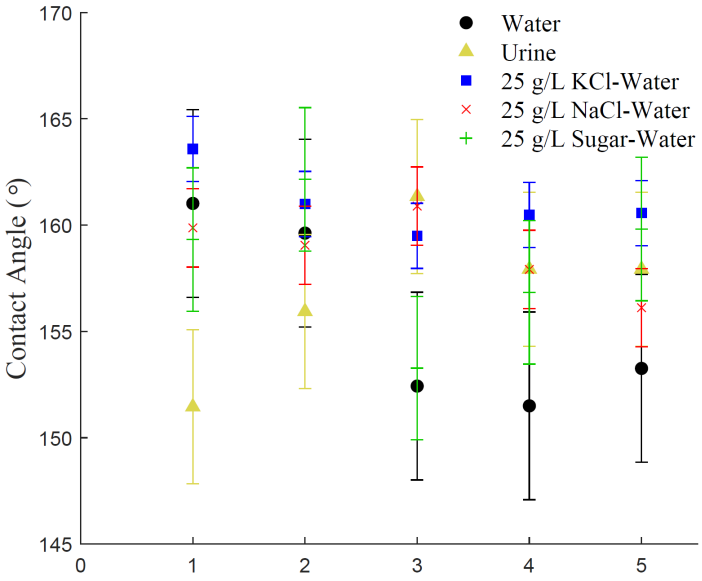

Figure 12: Contact angle results for water, urine, and aqueous mixtures on a superhydrophobic surface made of candle soot and Dome Magic™ PTFE spray.

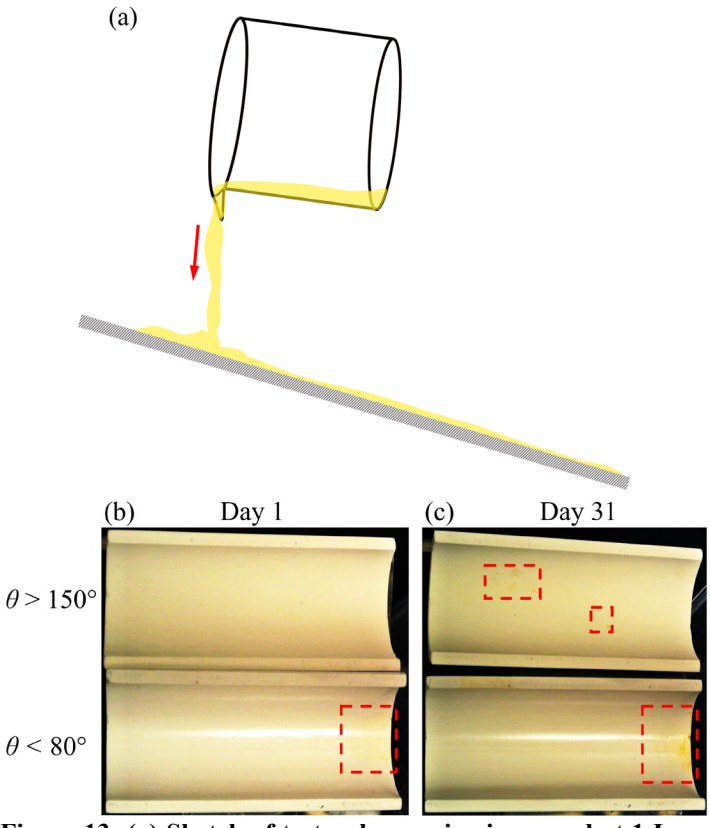

Figure 13: (a) Sketch of tests where urine is poured at 1 Lpm into a tilted PVC pipe. Images of the superhydrophobic (above) and non-hydrophobic (below) interior surfaces of PVC pipes after (b) 1 day and (c) 31 days of exposure. Red boxes highlight buildup of dry urine residue.

C. Non-Contact Distillation

A novel, non-contact, heat-driven distillation method has been investigated to address NASA's water recovery challenge.[93] The method exploits the Leidenfrost phenomenon to

perform distillation of droplet streams of waste-water. When a substrate's temperature is significantly higher than the liquid's boiling temperature, a droplet dispensed on the substrate will not undergo nucleate boiling, but will instead levitate on a layer of its own vapor. This vapor layer insulates the droplet from the heated substrate, reducing heat transfer to the liquid drop by orders of magnitude. Levitating droplets are not in contact with the surface, eliminating nucleation sites for bubble formation. This contact-free mode of distillation has potential utility for addressing the urine water recovery challenges in a fouling-free system.

The Leidenfrost distillation method is enhanced by superhydrophobic surfaces. Superhydrophobic surfaces have been shown to dramatically decrease the Leidenfrost point temperature of water.[94] Dynamic Leidenfrost impact temperatures have been observed to decrease from 206°C on an aluminum surface to as low as 130°C on a superhydrophobic surface.[93] Figure 14 shows a series of 15 Hz images taken of a 1.3 mL water droplet in microgravity impacting a superhydrophobic substrate held at 140°C. A Logan Shooter is used to eject the water droplet free of oscillations toward the heated substrate with a normal velocity of 13.0 cm/s and a perpendicular Weber number of 3.1. The droplet impacts the substrate and elastically rebounds without undergoing nucleate boiling. The reduction of Leidenfrost temperatures helps reduce energy consumption required for essentially non-contact Leidenfrost distillation. Superhydrophobic surfaces in conjunction with the Leidenfrost vapor layer separation provide an additional protection against contact between fluid and substrate.[93]

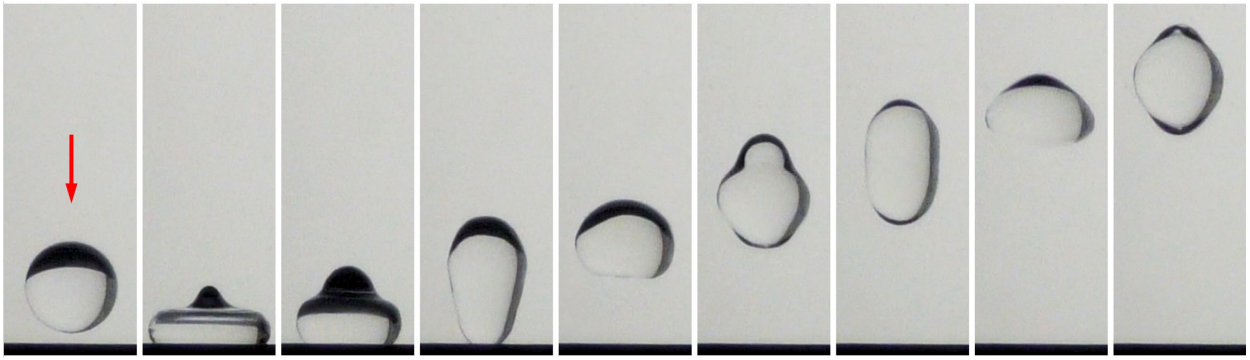

Figure 14: A sequence of 15 Hz images of a 1.3 mL water droplet impacting a planar superhydrophobic surface held at 140°C in a low-g drop tower test. The droplet is ejected using a passive Logan Shooter free of oscillations and normal to the substrate at 13.0 cm/s with a normal impact Weber number of 3.1.[95]

IV. Conclusion

The recent advances in easy-to-fabricate superhydrophobic surfaces are readily applicable for low-g demonstrations leading to practical applications in fluids handling aboard spacecraft. Such surfaces requiring simple production methods have gained significant attention in the past two decades. Desirable surface properties include thermal stability, corrosion resistance, wear resistance, bio-compatibility, and chemical stability, among others. Because such surfaces offer the potential for low-contact or even contact-free fluids handling aboard spacecraft, significant decreases in surface contamination might be achieved prolonging design life while reducing spares, mass, volume, costs, and crew time. Superhydrophobic surfaces offer a host of valued characteristics for spacecraft fluids systems including increased thermal stability, corrosion resistance, resistance to mechanical abrasion, and more. The use of superhydrophobic surfaces in a selection of demonstrative drop tower experiments have been briefly presented herein which identify a variety of large length scale interfacial microgravity fluid phenomenon ranging from jumping puddles, to rebounding droplets, to bouncing jets, to non-contact low-g distillation exploiting superhydrophobic surfaces at or above the Leidenfrost temperature. Such demonstrations suggest that current life support system applications susceptible to biofouling plumbing may benefit greatly from the immediate deployment of such surfaces. The utility and potential performance improvements of fluid-based systems for these surfaces is high per unit design effort. Further low-g demonstrations are encouraged as well as the development of a suite of flight certified superhydrophobic substrates that might be employed in the life support systems aboard spacecraft.

Acknowledgments

This work was supported in part by NASA Space Technology Research Fellowship titled Leidenfrost Driven Waste-Water Separator, September 15, 2017: CoTR, Jennifer Pruitt.[98]

References

[1]Marmur, A. (2004). The lotus effect: superhydrophobicity and metastability. *Langmuir*, *20*(9), 3517-3519.

[2]Wang, S., Liu, K., Yao, X., & Jiang, L. (2015). Bioinspired surfaces with superwettability: new insight on theory, design, and applications. *Chemical Reviews*, *115*(16), 8230-8293.

[3]Kumar, D., Li, L., & Chen, Z. (2016). Mechanically robust polyvinylidene fluoride (PVDF) based superhydrophobic coatings for self-cleaning applications. *Progress in Organic Coatings*, *101*, 385-390.

[4]Lai, Y., Huang, J., Cui, Z., Ge, M., Zhang, K. Q., Chen, Z., & Chi, L. (2016). Recent Advances in TiO2-Based Nanostructured Surfaces with Controllable Wettability and Adhesion. *Small*, *12*(16), 2203-2224.

[5]Wang, H., Zhu, Y., Hu, Z., Zhang, X., Wu, S., Wang, R., & Zhu, Y. (2016). A novel electrodeposition route for fabrication of the superhydrophobic surface with unique self-cleaning, mechanical abrasion and corrosion resistance properties. *Chemical Engineering Journal*, *303*, 37-47.

[6]Hejazi, I., Sadeghi, G. M. M., Jafari, S. H., Khonakdar, H. A., Seyfi, J., Holzschuh, M., & Simon, F. (2015). Transforming an intrinsically hydrophilic polymer to a robust self-cleaning superhydrophobic coating via carbon nanotube surface embedding. *Materials & Design*, *86*, 338-346.

[7]Bixler, G. D., & Bhushan, B. (2013). Fluid drag reduction with shark-skin riblet inspired microstructured surfaces. *Advanced Functional Materials*, *23*(36), 4507-4528.

[8]Bhushan, B., & Jung, Y. C. (2011). Natural and biomimetic artificial surfaces for superhydrophobicity, self-cleaning, low adhesion, and drag reduction. *Progress in Materials Science*, *56*(1), 1-108.

[9]Daniello, R. J., Waterhouse, N. E., & Rothstein, J. P. (2009). Drag reduction in turbulent flows over superhydrophobic surfaces. *Physics of Fluids*, *21*(8), 085103.

[10]Chiou, N. R., Lu, C., Guan, J., Lee, L. J., & Epstein, A. J. (2007). Growth and alignment of polyaniline nanofibres with superhydrophobic, superhydrophilic and other properties. *Nature Nanotechnology*, *2*(6), 354.

[11]Wang, N., Xiong, D., Deng, Y., Shi, Y., & Wang, K. (2015). Mechanically robust superhydrophobic steel surface with anti-icing, UV-durability, and corrosion resistance properties. *ACS Appl. Mt.-ls.*, *7*(11), 6260-6272.

[12]Boinovich, L. B., Emelyanenko, A. M., Emelyanenko, K. A., & Maslakov, K. I. (2016). Anti-icing properties of a superhydrophobic surface in a salt environment: an unexpected increase in freezing delay times for weak brine droplets. *Physical Chemistry Chemical Physics*, *18*(4), 3131-3136.

[13]Liu, K., Cao, M., Fujishima, A., & Jiang, L. (2014). Bio-inspired titanium dioxide materials with special wettability and their applications. *Chemical Reviews*, *114*(19), 10044-10094.

[14]Zheng, S., Li, C., Fu, Q., Hu, W., Xiang, T., Wang, Q., ... & Chen, Z. (2016). Development of stable superhydrophobic coatings on aluminum surface for corrosion-resistant, self-cleaning, and anti-icing applications. *Materials & Design*, *93*, 261-270.

[15]Zhang, B., Li, J., Zhao, X., Hu, X., Yang, L., Wang, N., ... & Hou, B. (2016). Biomimetic one step fabrication of manganese stearate superhydrophobic surface as an efficient barrier against marine corrosion and Chlorella vulgaris-induced biofouling. *Chemical Engineering Journal*, *306*, 441-451.

[16]Zhao, L., Liu, Q., Gao, R., Wang, J., Yang, W., & Liu, L. (2014). One-step method for the fabrication of superhydrophobic surface on magnesium alloy and its corrosion protection, antifouling performance. *Corrosion Science*, *80*, 177-183.

[17]Peres, R. S., Baldissera, A. F., Armelin, E., Alemán, C., & Ferreira, C. A. (2014). Marine-friendly antifouling coating based on the use of a fatty acid derivative as a pigment. *Materials Research*, *17*(3), 720-727.

[18]Wang, Q., Yu, M., Chen, G., Chen, Q., & Tian, J. (2017). Robust fabrication of fluorine-free superhydrophobic steel mesh for efficient oil/water separation. *Journal of Materials Science*, *52*(5), 2549-2559.

[19]Wang, G., Zeng, Z., Wang, H., Zhang, L., Sun, X., He, Y., ... & Xue, Q. (2015). Low drag porous ship with superhydrophobic and superoleophilic surface for oil spills cleanup. *ACS Appl. Mt.-It*, *7*(47), 26184-26194.

[20]Esmaeilirad, A. (2017). *Fabrication of robust superhydrophobic aluminium alloys and their application in corrosion protection* (Doctoral dissertation).

[21]Rezayi, T., & Entezari, M. H. (2017). Fabrication of superhydrophobic iron with anti-corrosion property by ultrasound. *Surface and Coatings Technology*, *309*, 795-804.

[22]Kota, A. K., Choi, W., & Tuteja, A. (2013). Superomniphobic surfaces: design and durability. *MRS bulletin*, *38*(5), 383-390.

[23]Shafrin, E. G., & Zisman, W. A. (1963). *Upper limits for the contact angles of liquids on solids* (No. NRL-5985). NAVAL RESEARCH LAB WASHINGTON DC.

[24]Quéré, D. (2008). Wetting and roughness. *Annu. Rev. Mater. Res.*, *38*, 71-99.

[25]Nishino, T., Meguro, M., Nakamae, K., Matsushita, M., & Ueda, Y. (1999). The lowest surface free energy based on− CF3 alignment. *Langmuir*, *15*(13), 4321-4323.

[26]Gao, X., & Jiang, L. (2004). Biophysics: water-repellent legs of water striders. *Nature*, *432*(7013), 36.

[27]Feng, X. Q., Gao, X., Wu, Z., Jiang, L., & Zheng, Q. S. (2007). Superior water repellency of water strider legs with hierarchical structures: experiments and analysis. *Langmuir*, *23*(9), 4892-4896.

[28]Su, Y., Ji, B., Huang, Y., & Hwang, K. C. (2010). Nature's design of hierarchical superhydrophobic surfaces of a water strider for low adhesion and low-energy dissipation. *Langmuir*, *26*(24), 18926-18937.

[29]Guo, Z., & Liu, W. (2007). Biomimic from the superhydrophobic plant leaves in nature: Binary structure and unitary structure. *Plant Science*, *172*(6), 1103-1112.

[30]Koch, K., Bhushan, B., Jung, Y. C., & Barthlott, W. (2009). Fabrication of artificial Lotus leaves and significance of hierarchical structure for superhydrophobicity and low adhesion. *Soft Matter*, *5*(7), 1386-1393.

[31]Feng, L., Li, S., Li, Y., Li, H., Zhang, L., Zhai, J., ... & Zhu, D. (2002). Super-hydrophobic surfaces: from natural to artificial. *Advanced Materials*, *14*(24), 1857-1860.

[32]Sun, Z., Liao, T., Liu, K., Jiang, L., Kim, J. H., & Dou, S. X. (2014). Fly-Eye Inspired Superhydrophobic Anti-Fogging Inorganic Nanostructures. *Small*, *10*(15), 3001-3006.

[33]Byun, D., Hong, J., Ko, J. H., Lee, Y. J., Park, H. C., Byun, B. K., & Lukes, J. R. (2009). Wetting characteristics of insect wing surfaces. *Journal of Bionic Engineering*, *6*(1), 63-70.

[34]Hasan, J., Webb, H. K., Truong, V. K., Pogodin, S., Baulin, V. A., Watson, G. S., ... & Ivanova, E. P. (2013). Selective bactericidal activity of nanopatterned superhydrophobic cicada Psaltoda claripennis wing surfaces. *Applied Microbiology and Biotechnology*, *97*(20), 9257-9262.

[35]Zhai, L., Berg, M. C., Cebeci, F. C., Kim, Y., Milwid, J. M., Rubner, M. F., & Cohen, R. E. (2006). Patterned superhydrophobic surfaces: toward a synthetic mimic of the Namib Desert beetle. *Nano Letters*, *6*(6), 1213-1217.

[36]Parker, A. R., & Lawrence, C. R. (2001). Water capture by a desert beetle. *Nature*, *414*(6859), 33.

[37]Dorrer, C., & Rühe, J. (2008). Mimicking the Stenocara Beetle Dewetting of Drops from a Patterned Superhydrophobic Surface. *Langmuir*, *24*(12), 6154-6158.

[38]Garrod, R. P., Harris, L. G., Schofield, W. C. E., McGettrick, J., Ward, L. J., Teare, D. O. H., & Badyal, J. P. S. (2007). Mimicking a Stenocara Beetle's back for microcondensation using plasmachemical patterned superhydrophobic− superhydrophilic surfaces. *Langmuir*, *23*(2), 689-693.

[39]Darmanin, T., & Guittard, F. (2014). Recent advances in the potential applications of bioinspired superhydrophobic materials. *Journal of Materials Chemistry A*, *2*(39), 16319-16359.

[40]Darmanin, T., Tarrade, J., Celia, E., & Guittard, F. (2014). Superoleophobic meshes with high adhesion by electrodeposition of conducting polymer containing short perfluorobutyl chains. *The Journal of Physical Chemistry C*, *118*(4), 2052-2057.

[41]Wenzel, R. N. (1936). Resistance of solid surfaces to wetting by water. *Industrial & Engineering Chemistry*, *28*(8), 988-994.

[42]Cassie, A. B. D., & Baxter, S. (1944). Wettability of porous surfaces. *Trans. of the Faraday Soc.*, *40*, 546-551.

[43]Gogolides, E., Ellinas, K., & Tserepi, A. (2015). Hierarchical micro and nano structured, hydrophilic, superhydrophobic and superoleophobic surfaces incorporated in microfluidics, microarrays and lab on chip microsystems. *Microelectronic Engineering*, *132*, 135-155.

[44]Liao, R., Zuo, Z., Guo, C., Yuan, Y., & Zhuang, A. (2014). Fabrication of superhydrophobic surface on aluminum by continuous chemical etching and its anti-icing property. *Applied Surface Science*, *317*, 701-709.

[45]Zhang, Y., Wu, J., Yu, X., & Wu, H. (2011). Low-cost one-step fabrication of superhydrophobic surface on Al alloy. *Applied Surface Science*, *257*(18), 7928-7931.

[46]Wu, R., Liang, S., Pan, A., Yuan, Z., Tang, Y., Tan, X., ... & Yu, Y. (2012). Fabrication of nano-structured super-hydrophobic film on aluminum by controllable immersing method. *Applied Surface Science*, *258*(16), 5933-5937.

[47]Li, X., Zhang, Q., Guo, Z., Shi, T., Yu, J., Tang, M., & Huang, X. (2015). Fabrication of superhydrophobic surface with improved corrosion inhibition on 6061 aluminum alloy substrate. *Applied Surface Science*, *342*, 76-83.

[48]Yang, J., & Li, W. (2013). Preparation of superhydrophobic surfaces on Al substrates and the anti-icing behavior. *Journal of Alloys and Compounds*, *576*, 215-219.

[49]Liu, W., Sun, L., Luo, Y., Wu, R., Jiang, H., Chen, Y., ... & Liu, Y. (2013). Facile transition from hydrophilicity to superhydrophilicity and superhydrophobicity on aluminum alloy surface by simple acid etching and polymer coating. *Applied Surface Science*, *280*, 193-200.

[50]Ruan, M., Li, W., Wang, B., Deng, B., Ma, F., & Yu, Z. (2013). Preparation and anti-icing behavior of superhydrophobic surfaces on aluminum alloy substrates. *Langmuir*, *29*(27), 8482-8491.

[51]Li, K., Zeng, X., Li, H., & Lai, X. (2015). A study on the fabrication of superhydrophobic iron surfaces by chemical etching and galvanic replacement methods and their anti-icing properties. *Appl. Surface Sci.*, *346*, 458-463.

[52]Lv, F. Y., & Zhang, P. (2014). Fabrication and characterization of superhydrophobic surfaces on aluminum alloy substrates. *Applied Surface Science*, *321*, 166-172.

[53]Li, P., Chen, X., Yang, G., Yu, L., & Zhang, P. (2014). Fabrication and characterization of stable superhydrophobic surface with good friction-reducing performance on Al foil. *Appl. Surface Science*, *300*, 184-190.

[54]Feng, L., Che, Y., Liu, Y., Qiang, X., & Wang, Y. (2013). Fabrication of superhydrophobic aluminium alloy surface with excellent corrosion resistance by a facile and environment-friendly method. *Applied Surface Science*, *283*, 367-374.

[55]Esmaeilirad, A., Rukosuyev, M. V., Jun, M. B., & van Veggel, F. C. (2016). A cost-effective method to create physically and thermally stable and storable super-hydrophobic aluminum alloy surfaces. *Surface and Coatings Technology*, *285*, 227-234.

[56]Liu, W., Sun, L., Luo, Y., Wu, R., Jiang, H., Chen, Y., ... & Liu, Y. (2013). Facile transition from hydrophilicity to superhydrophilicity and superhydrophobicity on aluminum alloy surface by simple acid etching and polymer coating. *Applied Surface Science*, *280*, 193-200.

[57]Sarkar, D. K., Farzaneh, M., & Paynter, R. W. (2008). Superhydrophobic properties of ultrathin rf-sputtered Teflon films coated etched aluminum surfaces. *Materials letters*, *62*(8-9), 1226-1229.

[58]Sun, Z., Liu, B., Huang, S., Wu, J., & Zhang, Q. (2017). Facile fabrication of superhydrophobic coating based on polysiloxane emulsion. *Progress in Organic Coatings*, *102*, 131-137.

[59]Agarwal, S., Horst, S., & Bognitzki, M. (2006). Electrospinning of fluorinated polymers: formation of superhydrophobic surfaces. *Macromolecular Materials and Engineering*, *291*(6), 592-601.

[60]Arukalam, I. O., Oguzie, E. E., & Li, Y. (2018). Nanostructured superhydrophobic polysiloxane coating for high barrier and anticorrosion applications in marine environment. *Journal of Colloid and Interface Science*, *512*, 674-685.

[61]Saadat-Bakhsh, M., Ahadian, H. R., & Nouri, N. M. (2017). Facile, robust and large-scale fabrication method of mechanically durable superhydrophobic PDMS/aerogel coating on fibrous substrates. *Cellulose*, *24*(8), 3453-3467.

[62]Cao, W. T., Liu, Y. J., Ma, M. G., & Zhu, J. F. (2017). Facile preparation of robust and superhydrophobic materials for self-cleaning and oil/water separation. *Colloids and Surfaces A: Physicochemical and Engineering Aspects*, *529*, 18-25.

[63]Li, C., Sun, Y., Cheng, M., Sun, S., & Hu, S. (2018). Fabrication and characterization of a TiO2/polysiloxane resin composite coating with full-thickness super-hydrophobicity. *Chemical Engineering Journal*, *333*, 361-369.

[64]Gao, S., Huang, J., Li, S., Liu, H., Li, F., Li, Y., ... & Lai, Y. (2017). Facile construction of robust fluorine-free superhydrophobic TiO2@ fabrics with excellent anti-fouling, water-oil separation and UV-protective properties. *Materials & Design*, *128*, 1-8.

[65]Lv, C., Wang, H., Liu, Z., Wang, C., Li, H., Zhao, Y., & Zhu, Y. (2017). A fluorine-free superhydrophobic PPS composite coating with high thermal stability, wear resistance, corrosion resistance. *Progress in Organic Coatings*, *110*, 47-54.

[66]Wu, Y., Jia, S., Wang, S., Qing, Y., Yan, N., Wang, Q., & Meng, T. (2017). A facile and novel emulsion for efficient and convenient fabrication of durable superhydrophobic materials. *Chemical Engineering J.*, *328*, 186-196.

[67]Lei, S., Shi, Z., Ou, J., Li, W., Qiao, G., & Yu, X. (2016). A facile process for preparing superhydrophobic PBZ-PTFE coating with excellent stable properties. *Applied Physics A*, *122*(12), 1011.

[68]Li, Y., Men, X., Zhu, X., Ge, B., Chu, F., & Zhang, Z. (2016). One-step spraying to fabricate nonfluorinated superhydrophobic coatings with high transparency. *Journal of Materials Science*, *51*(5), 2411-2419.

[69]Qahtan, T. F., Gondal, M. A., Alade, I. O., & Dastageer, M. A. (2017). Fabrication of water jet resistant and thermally stable superhydrophobic surfaces by spray coating of candle soot dispersion. *Scientific Reports*, *7*(1), 7531.

[70]Hancer, M., & Arkaz, H. (2015). A facile fabrication of superhydrophobic nanocomposite coating with contact angles approaching the theoretical limit. *Applied Surface Science*, *354*, 342-346.

[71]Wei, C., Tang, Y., Zhang, G., Zhang, Q., Zhan, X., & Chen, F. (2016). Facile fabrication of highly omniphobic and self-cleaning surfaces based on water mediated fluorinated nanosilica aggregation. *RSC Adv*, *6*(78), 74340-74348.

[72]Long, M., Peng, S., Yang, X., Deng, W., Wen, N., Miao, K., ... & Deng, W. (2017). One-Step Fabrication of Non-Fluorinated Transparent Super-Repellent Surfaces with Tunable Wettability Functioning in Both Air and Oil. *ACS Applied Materials & Interfaces*, *9*(18), 15857-15867.

[73]Liu, X., Xu, Y., Ben, K., Chen, Z., Wang, Y., & Guan, Z. (2015). Transparent, durable and thermally stable PDMS-derived superhydrophobic surfaces. *Applied Surface Science*, *339*, 94-101.

[74]Cai, Z., Lin, J., & Hong, X. (2018). Transparent superhydrophobic hollow films (TSHFs) with superior thermal stability and moisture resistance. *RSC Advances*, *8*(1), 491-498.

[75]Deng, X., Mammen, L., Butt, H. J., & Vollmer, D. (2012). Candle soot as a template for a transparent robust superamphiphobic coating. *Science*, *335*(6064), 67-70.

[76]Covelo, A., Menchaca, C., Flores, M., Rodríguez-Rojas, P., Hernandez-Gallegos, M., Meza, E. M., ... & Uruchurtu, J. (2017). Hydrophobic Coatings for Corrosion Control of Aluminum Heat Exchangers. In *New Technologies in Protective Coatings*. IntechOpen.

[77]Dryden Drop Tower Homepage: https://www.pdx.edu/dryden-drop-tower/

[78]Wollman, A., & Weislogel, M. (2013). New investigations in capillary fluidics using a drop tower. *Experiments in fluids*, *54*(4), 1499.

[79]Wollman A (2012) Capillarity-driven droplet ejection. Master's thesis, Portland State University. PermanentLink: http://archives.pdx.edu/ds/psu/8243

[80]Torres, L., Weislogel, M., Avhad, A., Tan, H., Large droplet generation by capillary migration in super-hydrophobic wedges, 33rd Annual Meeting of the American Society for Gravitational and Space Research, ID306, Seattle, Oct. 25-28, 2017.

[81]Attari, B., Weislogel, M., Wollman, A., Chen, Y., & Snyder, T. (2016). Puddle jumping: Spontaneous ejection of large liquid droplets from hydrophobic surfaces during drop tower tests. *Physics of Fluids*, *28*(10), 102104.

[82]Wollman, A., Weislogel, M., Wiles, B., Pettit, D., & Snyder, T. (2016). More investigations in capillary fluidics using a drop tower. *Experiments in Fluids*, *57*(4), 57.

[83]Schmidt, E. S., Weislogel, M. (2018). Electro-drop Bouncing in Low-gravity. Thesis, Portland State University.

[84]Torres, L., & Weislogel, M. (2019). Capillary migration of large confined drops in non-wetting wedges. Master's thesis, Portland State University (In press).

[85]Torres L., M. Weislogel, S. Arnold, Capillary migration of large confined super-hydrophobic drops in wedges, 69th Annual Meeting of the APS Division of Fluid Dynamics, Vol. 61-20, D36.00006, Portland, Nov. 20–22, 2016.

[86]Cardin, K., & Weislogel, M. (2019). Capillary migration of large confined drops in non-wetting wedges. Master's thesis, Portland State University (In press).

[87]Cardin, K., Weislogel, M.. "Rebound of Large Jets from Hydrophobic Surfaces in Low-Gravity." 71st Annual Meeting of the APS Division of Fluid Dynamics, M31.05, Atlanta, GA, November 18-20, 2018.

[88]Cardin, K., Weislogel, M.. "Capillary Fluidics: Discovery via Drop Tower." 42nd Committee on Space Research Scientiic Assembly, Pasadena, CA, July 14-22, 2018.

[89]Weislogel, M., Attari, B., Wollman, A., Cardin, K., Geile, J., Lindner, T.. "Big Hydrophobic Capillary Fluidics; Basically Water Ping Pong in Space." 69th Annual Meeting of the APS Division of Fluid Dynamics, L37.09, Volume 61, Number 20, Portland, OR, November 20-22, 2016.

[90]Chiaramonte, F. P., & Joshi, J. A. (2004). Workshop on Critical Issues in Microgravity Fluids, Transport, and Reaction Processes in Advanced Human Support Technology.

[91]Jones, H. W., & Kliss, M. H. (2010). Exploration life support technology challenges for the Crew Exploration Vehicle and future human missions. *Advances in Space Research*, *45*(7), 917-928.

[92]Thomas, E., & Muirhead, D. (2009). Impact of wastewater fouling on contact angle. *Biofouling*, *25*(5), 445-454.

[93]Rasheed, M. R., & Weislogel, M. (2019, July). On-Demand Non-Contact Distillation: Low-g Demonstrations of a Leidenfrost Waste-Water Processor. 49th International Conference on Environmental Systems (In press).

[94]Vakarelski, I. U., Patankar, N. A., Marston, J. O., Chan, D. Y., & Thoroddsen, S. T. (2012). Stabilization of Leidenfrost vapour layer by textured superhydrophobic surfaces. *Nature*, *489*(7415), 274.

[95]Rasheed, R., Weislogel, M., Large Length Scale Leidenfrost Phenomena: Recent Results from Drop Tower Experimentation, 34th Annual Meeting of the American Society for Gravitational and Space Research, ID-237, Bethesda, Oct. 31-Nov. 3, 2018.

[96]Ray, C. D., Salyer, B. H. (1999). *International Space Station ECLSS Technical Task Agreement Summary Report.*

[97]Holder Jr, D. W., Carter, D. L., & Hutchens, C. F. (1995). *Phase III integrated water recovery testing at MSFC: international space station configuration test results and lessons learned.* SAE transactions*, 821-833.*

[98]Original NSTRF Award Announcement, *"Leidenfrost Driven Waste Water Separator": https://www.nasa.gov/directorates/spacetech/strg/nstrf_2017/Leidenfrost_Driven_Waste-Water_Separator/*